Earth Surf. Dynam. Discuss., 1, 637–671, 2013
www.earth-surf-dynam-discuss.net/1/637/2013/
doi:10.5194/esurfd-1-637-2013

Earth Surface Dynamics
Discussions
Open Access

Field investigation of preferential fissure flow paths with hydrochemical analysis of small-scale sprinkling experiments

D. M. Krzeminska[1], T. A. Bogaard[1], T.-H. Debieche[2,4], F. Cervi[2], V. Marc[2], and J.-P. Malet[3]

[1]Water Resources Section, Faculty of Civil Engineering and Geosciences, Delft University of Technology, Delft, the Netherlands
[2]Université d'Avignon et des Pays de Vaucluse, UMR EMMAH 1114 INRA-UAPV, 33 rue Louis Pasteur, 84000 Avignon, France
[3]Institut de Physique du Globe de Strasbourg, CNRS UMR7516, Université de Strasbourg, Ecole et Observatoire des Sciences de la Terre, 5 rue Descartes, 67084 Strasbourg, France
[4]Water and Environment Team, Geological Engineering Laboratory, Jijel University, P.O. Box 98, 18000 Jijel, Algeria

Received: 6 October 2013 – Accepted: 17 October 2013 – Published: 30 October 2013

Correspondence to: D. M. Krzeminska (dkrzeminska@onet.eu)

Published by Copernicus Publications on behalf of the European Geosciences Union.

Abstract

The unsaturated zone largely controls groundwater recharge by buffering precipitation but at the same time providing preferential flow paths for infiltration. The importance of preferential flow on landslide hydrology is recognized in literature, but its monitoring and quantification remains difficult.

This paper presents a combined hydrological and hydrochemical analysis of small-scale sprinkling experiments with the aim to show the potential of such experiments for studying the spatial differences in dominant hydrological processes within a landslide. This methodology was tested in the highly heterogeneous black marls of the Super-Sauze landslide. The tests were performed in three areas characterised by different displacement rates, surface morphology and local hydrological conditions. Special attention was given to test the potential of small-scale sprinkling experiments to identify and characterise preferential flow patterns and dominating hydrological processes.

1 Introduction

In the last two decades, the understanding of hydrological processes in hillslopes has advanced due to improved monitoring techniques (McDonnell, 1990; Kirchner, 2003; Tromp-van Meerveld and McDonnell, 2006) and consequently, improved notion of mass movement dynamics (Haneberg, 1991; Uchida et al., 2001; Bogaard et al., 2004; Malet et al., 2005; de Montety et al., 2007; Wienhofer et al., 2011). Nevertheless, our knowledge is still incomplete, especially when it comes to infiltration and percolation processes, subsurface flow paths, and residence time of groundwater (Bogaard et al., 2004). The main difficulties stem from strong heterogeneity of hillslopes lithology and spatio-temporal variation of hydrological properties and dominant hydrological processes. This is particularly true when dealing with highly heterogeneous unconsolidated, partly weathered, silty-clay sediments, such as black marls. Additionally, in slow-moving clayey landslides, (constant) movement of sliding material results in the formation of fissures due to compression or extension depending on the differential movement and deformation rate (Anderson, 2005; Schulson and Duval, 2009; Niethammer et al., 2012, Walter et al., 2012; Stumpf et al., 2012). Here, the term “fissures” refers to geo-mechanically induced cracks that are filled or partly filled with reworked material. Accordingly, the term “preferential flow” refers to rapid water flow bypassing the bulk of the matrix (Beven and German, 1982) occurring through the areas of enhanced water fluxes due to the presence of fissures.

The presence of fissures creates so called “dual permeability” or “multiple permeability” systems. Dual permeability theory (Gwo et al., 1995; Greco et al., 2002; Šimůnek et al., 2003; Gerke, 2006; Jarvis, 2007) considers the porous medium as two (or more) interacting and overlapping but distinct continuum. The water flow occurs in both continua but it is the fracture continuum (macropore or fissure) that is the main transport medium, accommodating preferential flow. In this way, the presence of fissures may increase the rate of groundwater recharge (preferential vertical infiltration). On the other hand, it may increase the rate of drainage, which limits the building up of pore water pressure (preferential slope parallel drainage). However, when talking about dead-end fissures (disconnected fissure network, limited drainage capacity), they contribute to maintain high pore water pressures in the surrounding soils (McDonnell, 1990; Pierson, 1983; Van Beek and Van Asch, 1999; Uchida et al., 2001).

The quantification of groundwater recharge, especially by means of preferential flow, is a research challenge for an advanced understanding of hydrological systems in hillslopes and landslides (Savage et al., 2003; Coe et al., 2004; Weiler and McDonnell, 2007). However, the complexity of the processes and their high spatial variability make it very difficult to measure preferential flow in the field and to build up process models (Van Schaik, 2010). There are various experimental techniques that are used to gain insight into processes controlling preferential flow, e.g. dye tracing (Flury et al., 1994), tension infiltrometers (Angulo-Jaramillo et al., 1996) and continuous sampling of water drainage (e.g. multi sampler Wicky lysimeter; Boll et al., 1992). Nevertheless, a consis-

ESURFD
1, 637–671, 2013

tent measurement method for evaluating preferential flow is not yet achieved (Allaire et al., 2009).

The environmental tracing (Kabeya et al., 2007) and artificial tracing (Mali et al., 2007) in combination with hydrological survey are the most convenient investigation methods in field conditions. The experiments vary from laboratory tests (e.g. Allaire-Leung et al., 2000; Larsbo and Jarvis, 2006) to field experiments of different scales (e.g. Collins et al, 2002; Weiler and Naef, 2003; Mali et al., 2007; Kienzler and Naef, 2008). However, there is no plot scale field measurements dedicated to monitor and quantify preferential fissure flow, being a special case of macropores with apertures up to tens of centimetres.

The main objective of this research is to test the potential of small-scale ($1 \times 1\,m^2$) sprinkling experiment to identify, study and quantify the dominant hydrological processes within an active, highly heterogeneous landslide. The idea of using small-scale ($1 \times 1\,m^2$) sprinkling experiments rose after successful performing of large-scale (approximately $100\,m^2$) sprinkling tests in summer 2007 at the Super-Sauze landslide and the Laval landslide (Debieche et al., 2012; Garel et al., 2012). These two experiments gave valuable insight in the preferential infiltration and preferential later drainage processes in those unstable clay-shale hillslopes. However, due to the size and long duration, this kind of experiments are logistically and financially very demanding, and cannot be undertaken on a regular basis across the study area.

This paper presents the results obtained from three small-scale sprinkling tests performed on morphologically different areas of the persistently active Super-Sauze landslide (French Alps). The hydrological and hydrochemical observations were generalised into hydrological concepts and collated with current knowledge about the landslide.

ESURFD
1, 637–671, 2013

2 Methodology

2.1 Experimental design

The sprinkling experiments were performed with the use of sprinkling apparatus with one nozzle (1/4HH-10SQ), which was fixed at the top centre at around 2 m high. The apparatus was calibrated in order to provide a relatively homogeneous distribution of the sprinkling water over the $1 \times 1\,m^2$ experimental plot. Water supply was pumped in with regulated constant pressure (1.1 bars). The sprinkling was carried out in blocks of 15 min sprinkling and 15 min break with sprinkling intensity of approximately 20–30 mm $15\,min^{-1}$. This intensity is a trade off between a realistic sprinkling rate and the feasibility of the sprinkling equipment (pump and nozzle), and is high enough to ensure infiltration to both matrix and fissure compartments. To monitor actual sprinkling volume, and determine its distribution within the sprinkling plots, the rain gauges (5 per plot) were installed. In order to protect the experiment from wind disturbances and to minimize evaporation the experimental areas were covered with a tent. It is important to stress that the setup of the sprinkling experiment was designed to identify different patterns of the hydrological responses rather then being used for e.g. infiltration capacity measurement.

The $1 \times 1\,m^2$ sprinkling tests were carried out in two periods of 7–8 h sprinkling, composed of 14–17 sprinkling blocks (SB = 15 min rain + 15 min break), during two consecutive days. In this way, the first day of each sprinkling test started with dry initial conditions while the second one represented wet initial condition. The water used for the sprinkling tests was first collected in water tanks and blended with chemical tracers. The artificial tracing was introduced in order to get insights in the subsurface water flow paths and event and pre-event water mixing proportions. Therefore, the tracing was realised with two tracers: Br^- during the first day of experiment and Cl^- during the second day of experiment.

Within each sprinkling plot 4–5 piezometers were installed: one in the middle of the plot, two in the direction of expected (sub-)surface water movement (in the direction of fissures, if they were visible at the surface), and one upslope of the plot as the reference (Fig. 1b). The piezometers were made of PVC tubes with 0.50 m filters, covered with standard filter protection, surrounded by filter sand and closed with granular bentonite. All three experimental set-ups were built up two days before the sprinkling experiment started.

Groundwater responses were monitored manually every 15 min and with the use of automatic recording water pressure devices with a 3 min time resolution. The water for hydrochemical analyses was sampled every 1 h from all piezometers during the sprinkling experiment and one time per day for two consecutive days after the experiment. Additionally, the sprinkling plots were equipped with 1 m long access tubes for Theta Probes (PR1/6w-02, Delta-T Devices with reported accuracy of ±0.06 $m^3 m^{-3}$; Van Bavel and Nichols, 2002) in order to monitor changes in soil moisture profile at 6 depths (0.1, 0.2, 0.3, 0.4, 0.6 and 1.0 m). If the installation of Theta Probes was not possible (e.g. technical problems), the initial surface soil moisture (0–0.10 m depth) was measured with a manual field operated Time-Domain Reflectometry probe (TDR). The reported accuracy of the FOM TDR is ±0.02 $m^3 m^{-3}$ (IA PAS, 2006).

2.2 Analysis methodology

The soil column for water balance and for tracer mass balance calculation was bounded laterally by the 1 × 1 m^2 sprinkling surface area and vertically by the maximum depth of the piezometer installed in the center of each plot. The water balance of the sprinkling experiment for 7 or 8 h duration is:

$$P + \mathrm{GW}_{\mathrm{in}} = \mathrm{GW}_{\mathrm{out}} + \mathrm{OF} + E + \Delta S \tag{1}$$

where P is the precipitation (sprinkling), which represents the amount of sprinkling water, $\mathrm{GW}_{\mathrm{in}}$ and $\mathrm{GW}_{\mathrm{out}}$ are the groundwater inflow and outflow, OF is the overland flow, E is evaporation and ΔS is the change in storage over the duration of the sprinkling experiment.

ESURFD

1, 637–671, 2013

Moreover, a depletion curve analysis was applied in analogy of hydrograph recession analysis by applying the linear reservoir concept (Hornberger et al., 1991; Mikovari and Leibundgut, 1995; Sivapalan et al., 2002). Additionally, assuming that the groundwater level is a direct function of a change in drained volumes (therefore, a change in storage) it was possible to identify differences in types of storages based on occurrence of inflexion points in the drawdown curves. The time for depletion of the storages is indicated by a depletion factor. Depletion factor (K) is calculated for all segments of the drawdown curve defined by inflexion points using the empirical method explained by Linsley et al. (1982):

$$h_{t+\Delta t} = h_t \cdot e^{\frac{-\Delta t}{K}} \quad (2)$$

where h_t is the groundwater level at time t, and Δt the temporal resolution of groundwater level observations [min]. In general, the steeper part of the curve represents fast drainage, assumed to be preferential flow, whereas the gentle part represents slower drainage and represents matrix flow.

Besides qualitative description of the infiltration process the concentration of the conservative tracers (Br^- and Cl^-) was used to calculate the proportion of different water sources (event–pre-event water) using a two-component end-member mixing (EMMA) model. The EMMA model has been widely used for hydrological studies to separate the different contributions of streamflow (Christophersen and Hooper, 1992; Mulholland and Hill, 1997; Soulsby et al., 2003; James and Roulet, 2006; Cras et al., 2007). The end members are usually defined from the reservoir characteristics so mixing diagrams inform about the variable source areas of runoff. At the same time, they could be used to understand the flow processes which take place during infiltration. The mixing proportions ($\alpha(t)$ and $\beta(t)$) can be calculated by solving following equations:

$$\begin{cases} \alpha_1(t) \cdot C_{\mathrm{Br^-,EW1}} + \beta_1(t) \cdot C_{\mathrm{Br^-,PE}} = C_{\mathrm{Br^-}}(t) \\ \alpha_2(t) \cdot C_{\mathrm{Cl^-,EW2}} + \beta_2(t) \cdot C_{\mathrm{Cl^-,PE}} = C_{\mathrm{Cl^-}}(t) \\ \alpha_{1,2}(t) + \beta_{1,2}(t) = 1 \end{cases} \quad (3)$$

ESURFD
1, 637–671, 2013

where $C_{Br/Cl,EW/PE}$ and $C_{Br/Cl}(t)$ are tracer concentrations [$mg\,L^{-1}$] measured during the sprinkling experiment at different time (sampled from piezometers). PE and EW indicate the pre-event and event water, and the numbers indexes are related to first and second day of experiment, respectively.

Besides the added conservative tracers Br^- and Cl^-, also the sulphate concentration in groundwater prior the experiment could be used as an independent variable to define a "pre-event" end member ($C_{SO_4,PE}$). Sulphate is the major component of the groundwater chemistry and it can be used as tracer as long as the impact of the difference between groundwater and rainwater concentrations remains far larger than that of the water-rock interaction. When sprinkling is applied (EW), its sulphate content ($C_{SO_4,EW}$) can be considered as the second end member and the Eq. (3) can be attempted accordingly. The two estimated mixing proportions (for artificial and environmental tracers) for both experiments are plotted to analyse and validate the mixing assumption.

Furthermore, the simple mass balance equations were used (for Br^- and Cl^-) to estimate the most probable water (and tracer) flow paths and to restrain mixing processes:

$$V(t_{end}) = V_{PE} + V_{INF} - V_{SSF}$$
$$C_{Br^-/Cl^-}(t_{end}) \cdot V(t_{end}) = C_{Br^-/Cl^-,PE} \cdot V_{PE} + C_{Br^-/Cl^-,EW} \cdot V_{INF} - C_{Br^-/Cl^-}(t) \cdot V_{SSF} \quad (4)$$

where $V(t_{end})$, V_{PE}, V_{INF} and V_{SSF} are the estimated total water volume in the soil column at the end of sprinkling tests, the estimated volume of pre-event water, the estimated volume of infiltrated water (fraction of EW) and the estimated volume of subsurface flow (including exfiltration). The volume of pre-event (V_{PE}) is calculated based on initial groundwater level and initial soil moisture content:

$$V_{PE} = A \cdot (h_{t_0} \cdot n + (z - h_{t_0}) \cdot \theta_{ini}) \quad (5)$$

where A is the plot area [m^2], h_{t_0} is the groundwater level [m] observed before the experiment, n is average porosity [–], z is the depth of analysed soil column [m] and θ_{ini} is the initial soil moisture [–].

2.3 Characteristics of experimental plots

The experimental design was tested at the highly active Super-Sauze landslide (Fig. 1a), that covers 0.17 km^2 with an average slope of 25° and displacement velocities varying from 0.01 to 0.40 m day^{-1} depending on the season (Malet et al., 2002). The small-scale sprinkling experiments A and B are located in the upper part of the landslide which is the most active in terms of displacement rates, abrupt changes in groundwater levels throughout the season and changes in fissure density and openings (Fig. 1b). The experiment C is located in a relatively stable part of the landslide, but still at the direct contact with the most active area, and is representative of small displacement rates, small changes in groundwater levels throughout the season and no changes in fissure characteristics (Fig. 1b). As such, the three experimental plots shall present different hydrological responses (Malet, 2003; de Montety et al., 2007). All sprinkling experiments were localised in relatively flat areas with slope of 5–7°. The porosity values for the experimental plots were assumed to be 0.35, 0.38 and 0.30 in average for plot A, B and C, respectively, based on gravimetric measurements (Malet, 2003). The geomorphology of each plot is detailed below:

- Plot A is located in the active area near the crown consisting of relative fresh but heavily broken marl blocks and deposits (marly fragments of approximately 2 cm). There are wide (aperture of 0.07–0.15 m) undulating fissures observed on the surface (see Fig. 1b for the sketch), partly or totally filled with reworked marl fragments. The open depth of these fissures varies from 0.09 to 0.12 m.

- Plot B is located also in the very active area, at a secondary mudslide deposition area, that consists of gravel crust, characterized by coarse fragments (bigger than 2 mm) overlaying a finer matrix.There are wide open (apertures around 0.10 m) fissures present within the plot area with an open depth reaching 0.50 m (see Fig. 1b for the sketch).

ESURFD

1, 637–671, 2013

– Plot C is situated in the compacted, relatively stable, western part of the landslide and consists of fine grained with different rock fragments. No fissures are observed at the surface.

The depth of the piezometers is different at each area. Within plot A all piezometers were installed at approximately 2 m depth. Within plot B the piezometers depths are around 1 m due to the shallow groundwater level (see also Fig. 1b–c). Within plot C the depths of the piezometers were influenced by the presence of rock fragments in the soil and vary from 1.2 to 3.0 m.

3 Results of sprinkling experiments – hydrological and hydrochemical responses

Within each sprinkling plot different hydrological behaviours were observed. Figure 2a–c summarise the observed groundwater variation and tracer concentration patterns. Figure 3 shows the drawdown curves after the second day of sprinkling. For plot A and B the drawdown of the centrally-located piezometers was analysed (A1 and B1), while for plot C the analysis is carried out for piezometer C2 since the groundwater level observed in piezometer C1 was strongly influenced by water sampling.

3.1 Plot A

Plot A was a dry area with no groundwater observed within the first 2 m depth (depth A1) before the experiment started. The mean initial volumetric water content of the top soil layer (up to 0.30 m depth), was 0.12 with standard deviation of 0.03. In response to the applied sprinkling neither overland flow nor subsurface runoff was observed. The groundwater fluctuation in A1 showed a very fast vertical movement of water (approximately ±0.25–0.30 m in 15 min). Moreover, the drawdown after each day of sprinkling lasted four hours only (Fig. 2a).

ESURFD
1, 637–671, 2013

In A3, located in the direction of the surface fissures, the groundwater level started to react during the first day after fourth sprinkling block (SB-04). In A2, located downslope of the sprinkling plot but not in the direction of the surface fissures, the groundwater reaction started only during the second day after the fifth sprinkling block (SB-05). There was no response observed in A7.

The soil moisture variation observed in the soil profile in θ_{A2} (approximately 1 m distance from the sprinkling area) are negligible. In θ_{A1} no changes were observed in the first 0.60 m of soil profile. At 1 m depth soil moisture increased till saturation over the two days of the sprinkling experiment.

The tracer concentration in the piezometers gradually increased with cumulated amount of applied sprinkled water. Similar to the hydrological responses, the most intense changes were observed in A1, reaching 84 % (first day) and 93 % (second day) of applied tracer concentration at the end of each 7–8 h sprinkling. Moreover, tracer concentration decreased during the recession phase. At the start of the second day, Br^- concentration had nearly dropped back to the initial value. The same trend was observed for Cl^- during the second day. The tracer concentration in A2 and A3 followed the trend observed in A1, with the maximum measured tracer concentration reaching 26–38 % (first day) and 55–71 % (second day) of applied concentration for A3 and A2, respectively. It is important to note that in plot A, on the second day of experiment Br^- was applied during the first four sprinkling blocks (SB-01 to SB-04) with very high concentration (461 mg l^{-1}). This incident determined the behaviour of Br^- concentration at the beginning of the second day of sprinkling: the maximum concentration of Br^- was observed after SB-06 in A1, after SB-08 in A2, and after SB-12 in A3.

3.2 Plot B

Plot B was located at an area with shallow groundwater level (0.35–0.55 m below the surface). The average initial volumetric water content in the first 0.30 m of the soil was 0.25 with standard deviation of 0.07. During the sprinkling experiment an increase of groundwater level was observed only in B1 and B3 and they fluctuated ±0.07 m on

Discussion Paper | Discussion Paper | Discussion Paper | Discussion Paper |

ESURFD

1, 637–671, 2013

average, in response to single sprinkling block. No groundwater level changes in B2 and B6 were registered and no changes in soil moisture content in θ_{B1} or θ_{B2} (located within approximately 1m distance from $1 \times 1\,m^2$ sprinkling plot) were observed.

The exfiltrating subsurface runoff was measured around 1–1.5 m downslope of the experimental plot. The volume of subsurface runoff per sprinkling block increased with time. During the first day, it started with $15.9 \times 10^{-3}\,m^3$ for SB-05 and reached $18.3 \times 10^{-3}\,m^3$ for SB-14. During the second day, it ranged from $11.4 \times 10^{-3}\,m^3$ (for SB-01) to $19.5 \times 10^{-3}\,m^3$ (for SB-14).

In B1 and B3 the relative Br^- concentration rose quickly and reached 67 % and 93 % maximum respectively at the end of the first day. Moreover, it remained at a high level in-between two days of sprinkling (Fig. 2b). Similar tracer concentration behaviour was observed during the second day of the experiment, when chloride was applied. The observed Br^- concentration gradually decreased while the Cl^- concentration increased reaching 58 % (B1) and 99 % (B3) of applied concentration. The Cl^- concentration remained high (in B1 58 % and in B3 68 % of applied concentration) even 20 h after the end of the experiment. It is noteworthy that the concentration of Br^- and Cl^- is most of the time higher in B3 than in B1 and that the tracer concentration in the subsurface runoff equals (first day) or almost equals (second day; 81–99 %) that of the sprinkling water.

3.3 Plot C

Plot C had wetter initial conditions: the initial groundwater level was around 0.75–1.00 m below surface and the initial volumetric water content varied between 0.20 and 0.25 (0.23 in average) in the first 0.10 m of the soil. In contrast to the dynamics observed in plot A, around 75 % of the sprinkling water left the soil column as overland flow. Moreover, during the entire experiment ponding was observed within the $1 \times 1\,m^2$ plot.

The groundwater level observed in C1 and C2 respond similarly: an increase of groundwater level up to 0.20 m (for C1) and 0.05 m (for C2) below surface and fluctu-

ESURFD

1, 637–671, 2013

Field investigation of preferential fissure flow paths

D. M. Krzeminska et al.

ations of about 0.20 m after each 15 min of sprinkling. The drawdown observed in C1 stopped after 4 h whereas in B2 it took around 12 h after the sprinkling experiment. C3 showed 0.03–0.07 m groundwater level fluctuation and no response took place in C5 and C6. The groundwater level in the soil column went back to its initial stage within 12 h after the sprinkling ceased.

In C1 the relative concentration of Br^- reached approximately 43–49 % of the applied tracer concentration and was around constant during the first day of sprinkling. At the start of the second day Br^- relative concentration was 31 % and it rose again up to 50 % as soon as new sprinkling water (without Br^-) was applied (Fig. 2c). Similar trends were observed for C2, with the maximal tracer concentration reaching 28 % and 40 % of applied concentration for the first and second day, respectively. There was no tracer found in C3.

During the second day of the sprinkling experiment, the Cl^- concentration showed very limited increase in C1 but a gradual increase up to around 50 % of the applied concentration in C2. The Cl^- concentration decreased after the second day. However, in C2 it remained relatively high even 20 h after the experiment (300 mg L^{-1}). Again, no tracer was found in C3.

4 Discussion of experimental results and model conceptualisation

4.1 Water balance and tracer mass balance analysis

The water budget was calculated for each day of the sprinkling experiment form the beginning of the first sprinkling block (SB-01) till the end of the observed drawdown in the centrally located piezometer. As a first approximation the water balance components were estimated based on the assumption that the whole experimental area ($1 \times 1\ m^2$) is hydrologically active, meaning all water stored in the soil column is mobile and full mixing of pre-event water and event water occurs. The groundwater flow variations were assumed to be only due to infiltrating sprinkling water over the experimental

ESURFD
1, 637–671, 2013

plot (Fig. 4). This means we assume no change in overall groundwater flow and no change in deep percolation (plot B and C) due to the sprinkling activity. In case of plot A, where no groundwater level was observed before and short after the experiment, the direction of the estimated subsurface flow cannot be determined so the subsurface flow comprises both vertical deep percolation (Pe) and lateral flows (SSF). The volume of pre-event (V_{PE}) water was estimated based on Eq. (7), and the volume of infiltrated water (V_{INF}) was calculated as: $V_{\mathrm{EW}} - V_{\mathrm{OF}}$. The volume of subsurface fluxes (V_{SSF}), which comprises all subsurface fluxes, was estimated using the measured groundwater level responses to the sprinkling blocks and the change in storage ΔS was calculated as: $V_{\mathrm{INF}} - V_{\mathrm{SSF}}$. Evaporation ($E$) is assumed to be negligible as the sprinkling plots were covered with a tent. Table 1 shows the measured ($^{\mathrm{m}}$) and estimated ($^{\mathrm{e}}$) water balance components.

The tracer mass balance analysis was performed in order to evaluate the assumption of water mobility and full mixing within the soil column. The bromide and chloride masses were calculated from the chemical measurements and corresponding water volumes. The tracer mass remaining in the soil column was calculated in two ways: (1) based on the tracer mass balance and (2) based on the measured tracer concentration in the groundwater at the end of the sprinkling experiments. The differences between the two allowed us to evaluate the mixing assumption; the percent of the experimental area that is hydrological active (x) was estimated based on the following equation:

$$\begin{aligned} &C_{\mathrm{Br^-/Cl^-}}(t_{\mathrm{end}}) \cdot V(t_{\mathrm{end}}) = x \cdot C_{\mathrm{Br^-/Cl^-,PE}} \cdot V_{\mathrm{PE}} + C_{\mathrm{Br^-/Cl^-,EW}} \cdot V_{\mathrm{INF}} - x \cdot C_{\mathrm{Br^-/Cl^-}}(t) \cdot V_{\mathrm{SSF}} \\ &V(t_{\mathrm{end}}) = x \cdot V_{\mathrm{PE}} + V_{\mathrm{INF}} - x \cdot V_{\mathrm{SSF}} \end{aligned} \quad (6)$$

It is important to note that V_{PE} and V_{SSF} are estimated based on groundwater level observation multiplied by the (hydrologically active) area of the experiment.

Table 2 shows tracer mass balance component and is subdivided in two parts: first, the results based on the assumption that the whole soil column is hydrologically active (i.e. full mixing), second the results taking into account a percentage of the soil column that is hydrologically active.

ESURFD

1, 637–671, 2013

Furthermore, the influence of porosity values was evaluated. Increasing or decreasing the average porosity with 0.01 and 0.02 results in changes in the water balance components. There is limited influence of porosity on the estimated volume of pre-event water: no changes in plot A (since there was no groundwater before the experiment), ±5 % in plot B and ±3 % in plot C. The volume of subsurface flow is more sensitive for changes in soil porosity. It varies between ±35 % in plot A and ±24 % in plot C. Within plot B the change in subsurface flow volume expressed in percentage terms is also significant (between +11 % and −55 %) but it corresponds to relatively low absolute values (0.05–0.1 m^3). Consequently, the changes in volume of water stored in the soil column at the end of experiment are the highest for plot A (between −23 % and +44 %) and relatively limited for plot B (±7 %) and plot C (±14). The influence of porosity changes on calculated percentage of hydrologicaly active area (Eq. 6) is limited to maximum ±2 %.

4.2 Hydrological and hydrochemical observation

Clearly, a diverse spectrum of results emerges from the experiments. However, the results also show interesting similarities. The sprinkling water infiltrates into the top soil through both matrix and preferential (fissure) flow paths. Once water entered into the soil the plots show basically two types of drainage. First groundwater level depletes fast and slows down after 15–90 min. Interestingly, fast infiltration and fast drainage do not coincide. Plot A has both fast infiltration and fast drainage (both in first and second stage), whereas plot B shows high infiltration capacity but the second reservoir shows the slowest depletion of the stored subsurface water. Plot C has low infiltration rate but seems to drain the infiltrated water relatively smoothly.

The tracer information shows similarities with the groundwater patterns. Both bromide and chloride concentrations rise reaching almost the initial concentration of the sprinkling in the centre of plot A and around 60 % of the initial concentration of the sprinkling in the centre of plot B within the duration of the experiment. In plot C both tracers reach maximum 0.5 relative concentration indicating more mixing with pre-event water.

ESURFD
1, 637–671, 2013

The location of highest relative concentration is in the centre for plot A and downslope of plot B (in B3). Plot C results are again a bit more diverse, both piezometers C1 and C2 show mixing of sprinkling water with pre-event water for the first day but only the downslope located C2 shows a significant increase of chloride concentration during the second day experiment.

The results of the EMMA model underline the differences in mixing processes and their dynamics observed per plot (Fig. 5). For all plots the relation between mixing proportion estimated based on both applied tracer and sulphate concentrations do not follow the 1 : 1 line exactly. This can be an effect of soil–water interaction (dissolution of pyrite). This can be partly due to the uncertainty on the PE sulphate concentrations estimates which may vary quite a lot over short distances. Within plot A and B the mixing processes are clear: the mixing proportions change progressively during the sprinkling experiment from 0 % to more than 90 % (plot A) or around 70 % (plot B) for both tracers and sulphate. In plot C the mixing proportions increase during the first day but they are limited to 64 %. Moreover, in plot A and B, the artificial and environmental tracers behave similar over the two days sprinkling experiment showing that mixing processes can be explained with two end-member only: mixing of event water with pre-event water. This is also the case for the first day in plot C. During the second day of the experiment a sharp dilution of sulphate was observed in C1 while Cl^- concentration remained low and Br^- concentration increased. This indicates that in plot C, both event waters (EW1 during first day and EW2 during second day of sprinkling) contributed independently in mixing with pre-event water. However, it is important to stress that EMMA results are based only on tracer concentrations and give relative mixing proportion and do not give the absolute mass of mixed tracers.

The three plots show different spatial responses. In case of plot A three piezometers show a response in water level and in tracer concentration. In plot B and C only two piezometers react to the sprinkling in groundwater level and water quality. This suggests the plot B and C have structured flow paths whereas plot A is more permeable in all directions. Subsurface flow often follows the slope gradient, however, the presence of fissures and macroporosity (plot A and B) strongly influence flow direction.

Based on the interpretation of the sprinkling experiment, three types of hydrological behaviour are conceptualised:

- Fast input – fast output (plot A) – very fast infiltration as well as fast drainage.
- Fast input – slow output (plot B) – fast infiltration but very slow drainage
- Fast but limited input – moderate output (plot C) – limited infiltration and relatively slow drainage (when compared with plot A).

4.2.1 Concept 1: fast input – fast output

Plot A represents a fast input-output type of hydrological response: the very fast response to the onset of sprinkling as well as sudden groundwater level drop after sprinkling is finished. The sharp groundwater level decrease in A1 (see Fig. 3) after the end of the sprinkling test is an indication of drainage from a highly permeable fraction of the subsurface, e.g. the fissure fraction. Moreover, the second part of the depletion curve is quite rapid as well, indicating that also the matrix fraction is highly permeable. The very high permeability is confirmed by the fact that groundwater responses are observed not only in the centre of the experimental plot (A1) but also in two directions downslope: relatively quick response in A3 (direction of fissures observed on the surface) and delayed in A2.

There is 0.7 m^3 of pre-event water (approximately 33–36 % of maximal storage capacity) storage in the soil column. Of this pre-event water, 50–54 % could mix and readily move with the infiltrating sprinkling water (Tables 1 and 2). The incident with the accidentally application of high concentration Br^- at the beginning of the second day proofs the dominance of fast preferential flow through the plot and short residence times of water within the soil column.

ESURFD
1, 637–671, 2013

Field investigation of preferential fissure flow paths

D. M. Krzeminska et al.

4.2.2 Concept 2: fast input – slow output

The hydrological responses in plot B can be described as fast input – delayed output. The presence of a largely open (up to 14 cm) fissure system influences the distribution of infiltrating water. However, more than 70 % of the infiltrated water is flowing out of the soil column and exfiltrating downslope. The observed hydrological response is a combination of fast vertical infiltration, fast subsurface flow and much slower matrix flow. The shape of the drawdown curve (Fig. 3) also indicates the combination of mainly preferential flow and some matrix flow.

The behaviour of the tracer concentration indicates complex mixing processes in plot B. The changes in the Br^- and Cl^- concentration also show that infiltrating water of the first day replaced the pre-event water and is temporarily stored till the new source of water (sprinkling of second day) appears. The relatively low concentration of tracer in B1 shows that a significant amount of pre-event water (approximately 80–84 % of maximum storage) is stored in the matrix and 24–61 % of this water is involved in mixing process (Tables 1 and 2). The spatial distribution of tracer concentration (lower concentration in B1, higher in B3 and in subsurface flow) indicates a well structured subsurface (including fissure system) that can provide direct drainage for infiltrated water. The fast flow domain is isolated from the matrix (no or poor connection). When the groundwater level is high a well connected preferential flow system becomes active and the applied water drains directly ($K_{1,\mathrm{B}}$; Fig. 3). However, once the water level has dropped several centimetres the drainage stopped (e.g: dead – end fissure) and the system maintains high groundwater levels for several hours ($K_{2,\mathrm{B}}$; Fig. 3). The last drainage phase ($K_{3,\mathrm{B}}$; Fig. 3) can be interpreted as matrix flow after saturation connecting the wet fissure areas.

4.2.3 Concept 3: fast but limited input – moderate output

The general observation of the water balance component (Table 1) and drawdown curves (Fig. 3) indicates that plot C represents matrix-like infiltration behaviour, however, influence of preferential flow cannot be neglected. Significant drainage at the end of each 15 min of sprinkling and depletion constant for the steep part of depletion curve (K_{1C}) almost three times higher than the one for gentle second part of the curve (K_{2C}) indicates the presence of preferential flow paths (fissures, macropores) that influences the hydrological behaviour at studied scale.

There is significant amount of pre-event water (approximately 92–94 % of maximum storage) is stored in the soil column. The tracer mass balance for the first day of the experiment (Table 2) indicates that only around 16–18 % of the pre-event water stored in the subsurface is actively mixed with the infiltrated sprinkling water. The opposite conclusion can be drawn when analysing the mass balance for the second day of the sprinkling experiment. Under the assumption that all infiltrated sprinkling water is stored in the 1 × 1 m^2 plot, a double amount of pre-event water should be involved in mixing processes in order to match the measured Cl^- concentration in C1. However, the concentration of Cl^- in C2 (located outside the sprinkling plot) indicates that there is significant amount of tracer stored outside the experimental plot due to surface ponding and subsurface water flow. Moreover, assuming that the hydrologically active area during the second day of the experiment is the same as during the first day of experiment (around 20 %), only 1–2 % of infiltrated tracer mass is enough to reach the measured tracer concentration in the groundwater at the end of experiment. This indicates the presence of preferential drainage. Nevertheless, the presence of Br^- in C1 (middle of the sprinkling plot) during the second day, when only Cl^- was applied, confirms that matrix flow dominates in the area and piston flow processes occurred. The rise of the Br^- concentration, in both C1 and C2, observed at the beginning of the second day of sprinkling might be explained by the tracer settled over soil surface during water ponding during first day of sprinkling mobilised by "new" sprinkled water.

4.3 Discussion of conceptual models for the Super-Sauze landslide

The improvement of hydrological modelling of the Super-Sauze landslide is not a direct aim of this paper: the small number of sprinkling experiments and their small scale in

ESURFD
1, 637–671, 2013

relation to the landslide area 0.17 ha, is not sufficient to cover the whole landslide and the findings can not yet be up-scaled into a complete distributed hydrological concept of the landslide.

However, the components of the hydrological system, identified based on small-scale sprinkling tests, are in line with the conceptual model of the Super-Sauze landslide proposed by Malet et al. (2005) and deMontety et al. (2007). The former proposed a distributed conceptual model of hydrological behaviour of Super-Sauze landslide dividing the Super-Sauze landslide into hydro-geomorphological units (Fig. 1a). The upper unit (HG1), where plot A and B are located, is very active and characterised by very rapid responses and large groundwater level fluctuation (up to 0.5 m) at the event scale. The western part of upper unit (HG3), were plot C is located, is the most stable part of the landslide, with very limited groundwater level fluctuation (centimetres). Our results confirm this hydrological concept, but they also stress clear differences in hydrological response in the upper unit (Fig. 6) which was not presented as clearly by Malet et al. (2005). However, it is important to note that the hydrochemical behaviour observed in "plot C" is strongly influenced by the presence of small fissure and cannot be compared with general hydrological concept of Malet et al. (2005).

The hydrological interpretation of the Super-Sauze landslide presented by deMontety et al. (2007) and based on the long term observation of spatial distribution of major cations and anions defines dominant hydrological processes along the landslide profile: the upper part of the landslide (directly below the main scarp) is the "transition" zone while the middle part of the landslide is dominated by preferential flow. This is in agreement with our observed fast input – fast output behaviors in plot A and fast input – slow output behavior in plot B. The stable part of the landslide, where the plot C was located, was not considered in the work of deMontety et al. (2007). While deMontety et al. (2007) stressed the limitation of their investigation having only qualitative assessment of the water fluxes and the need for more detailed investigations, our experiments show the potential for more quantitative analyses of the components of the hydrologi-

ESURFD
1, 637–671, 2013

cal processes acting on the landslide and extension of the conceptual model with the identification of surface hydrological processes such as exfiltration and runoff.

Lastly, our results are comparable with the large-scale sprinkling experiment performed for more than one week at one location (in the area where plot B was located) at the Super-Sauze landslide (Debieche et al., 2012). Our results confirm that hydrodynamic and hydrochemical responses can not be fully inferred from surface area characteristics only. The sprinkling water infiltrates into the soil both through the matrix and preferential flow paths. The groundwater flow follows the overall slope direction but the presence of fissures and subsurface structures strongly influences the exact direction of the subsurface water flow. Moreover, unweathered marly blocks, characterised with relatively low permeability, decrease the percolation rate and create area of limited hydrological activity.

5 Conclusions

This paper shows the potential of combined hydrological and hydrochemical analysis of small-scale $1 \times 1\,m^2$ sprinkling experiments to study the spatial differences in hydrological response to precipitation input. The approach was applied at the specific environment of highly heterogeneous Super-Sauze landslide (French Alps).

Dual or multiple permeability systems can be found in many hillslopes and they steer the hydrological dynamics of the hillslope. In such cases, laboratory tests for hydraulic soil parameters are insufficient and in-situ measurements or experiments are necessary. Small-scale sprinkling experiments performed with the use of artificial tracer and in-situ observations of hydrological and hydrochemical response showed to be very effective in unravelling complex hydrological systems. The advantage of two days sprinkling experiment is also clear: it allows to perform more in-depth analysis of mixing processes (pre-event – infiltrated water). They confirm that presence of fissures increases the vertical infiltration rate and controls the direction of subsurface water flow (e.g. McDonnell, 1990; Uchida et al., 2001). Furthermore, our results support the find-

ESURFD
1, 637–671, 2013

ings of, for example, Trojan and Linden (1992), Zehe and Fluhler (2001), Weiler and Naef (2003), that antecedent water storage influences the initiation of preferential flow.

Presented experiments are relatively inexpensive, can be deployed throughout the landslide area and do not need long-term monitoring programs. This paves the road for more widespread application in order to better understand the spatial differences and similarities of hydrological processes across a landslide area. In order to extend the application of small-scale sprinkling experiments and to overcome current shortcomings the following should be considered:

- detailed measurements of soil characteristics, their heterogeneity in the analyzed soil profile, and their high temporal resolution monitoring during the sprinkling experiment;

- applying non-destructive measure to provide more detailed characteristics of subsurface fissure system, especially in vertical directions. Grandjean et al. (2012) and Travelletti et al. (2012) presented promising results based on seismic azimuth tomography or ERT measurements. However, both methodologies need further improvement to provide unique characteristics of subsurface flow paths.

Although we performed only a limited amount of experiments, we showed that small-scale sprinkling experiments were capable of capturing and monitoring the hydrological processes across the landslide. Moreover, they show potential for quantifying of subsurface flow process.

Acknowledgements. This work was supported by the European Commission within the Marie Curie Research and Training Network "*Mountain Risks: from prediction to management and governance*" (2007–2010, Contract MCRTN-035798) and by the French National Research Agency (ANR) within the project "Ecou-Pref – *Ecoulements préférentiels dans les versants marneux*" (Contract ANR05-ECCO-007-04).

References

Allaire, S. E., Roulier, S., and Cessna, A. J.: Quantifying preferential flow in soils: a review of different techniques, J. Hydrol., 378, 179–204, 2009.

Allaire-Leung, S. E., Gupta, S. C., and Moncreif, J. F.: Water and solute movement in soil as influenced by macropore characteristics: I. Macropore continuity, J. Contam. Hydrol., 41, 283–301, 2000.

Anderson, L.: Fracture Mechanics: Fundamentals and Applications, 3rd Edn., Taylor & Francis, 2005.

Angulo-Jaramillo, R., Gaudet, J.-P., Thony, J.-L., and Vauclin, M.: Measurement of hydraulic properties and mobile water content of a field soil, Soil Sci. Soc. Am. J., 60, 710–715, 1996.

Beven, K. and Germann, P.: Macropores and water flow in soils, Water Resour. Res., 18, 1311–1325, 1982.

Bogaard, T. A., Buma, J. T., and Klawer, C. J. M.: Testing the potential of geochemical techniques for identifying hydrological systems within landslides in partly weathered marls, Geomorphology, 58, 323–338, 2004.

Boll, J., Steenhuis, T. S., and Selker, J. S.: Fiberglass wicks for sampling of water and solutes in the vadose zone, Soil Sci. Soc. Am. J., 56, 701–707, 1992.

Christophersen, N. and Hooper, R. P.: Multivariate analysis of stream water chemical data – the use of principal component analysis for the end-member mixing problem, Water Resour. Res., 28, 99–107, doi:10.1029/91WR02518, 1992.

Coe, J. A., Michael, J. A., Crovelli, R. A., Savage, W. Z., Laprade, W. T., and Nashem, W. D.: Probabilistic assessment of precipitation-triggered landslides using historical records of landslide occurrence, Seattle, Washington, Environ. Eng. Geosci., 10, 103–122, 2004.

Collins, R., Jenkins, A., and Harrow, M.: The contribution of old and new water to a storm hydrograph determined by tracer addition to a whole catchment, Hydrol. Process., 14, 701–711, 2000.

Cras, A., Marc, V., and Travi, Y.: Hydrological behaviour of sub-Mediterranean alpine headwater streams in a badlands environment, J. Hydrol., 339, 130–144, doi:10.1016/j.jhydrol.2007.03.004, 2007.

Debieche, T.-H., Bogaard, T. A., Marc, V., Emblanch, C., Krzeminska, D. M., and Malet, J.-P.: Hydrological and hydrochemical processes observed during a large-scale infiltra-

tion experiment at the Super-Sauze mudslide (France), Hydrol. Process., 26, 2157–2170, doi:10.1002/hyp.7843, 2012.
De Montety, V., Marc, V., Emblanch, C., Malet, J.-P., Bertrand, C., Maquaire, O., and Bogaard, T. A.: Identifying the origin of groundwater and flow processes in complex landslides affecting black marls: insights from a hydrochemical survey, Earth Surf. Proc. Land., 32, 32–48, 2007.
Flury, M., Fluhler, H., Jury, W. A., and Leuenberger, J.: Susceptibility of soils to preferential flow of water: a field study, Water Resour. Res., 30, 1945–1954, 1994.
Garel, E., Marc, V., Ruy, S., Cognard-Plancq, A.-L., Klotz, S., Emblanch, C., and Simler, R.: Large scale rainfall simulation to investigate infiltration processes in a small landslide under dry initial conditions: the Draix hillslope experiment, Hydrol. Process., 26, 2171–2186, doi:10.1002/hyp.9273, 2012.
Gerke, H. H.: Preferential flow descriptions for structured soils, J. Plant Nutr. Soil Sc., 169, 382–400, 2006.
Grandjean, G., Bitri, A., and Krzeminska, D. M.: Characterisation of a landslide fissure pattern by integrating seismic azimuth tomography and geotechnical testing, Hydrol. Process., 26, 2120–2127, doi:10.1002/hyp.7993, 2012.
Greco, R.: Preferential flow in macroporous swelling soil with internal catchment, model development and applications, J. Hydrol., 269, 150–168, 2002.
Gwo, J. P., Jardine, P. M., Wilson, G. V., and Yeh, G. T.: A multiple-pore-region concept to modeling mass transfer in subsurface media, J. Hydrol., 164, 217–237, 1995.
Haneberg, W. C.: Observation and analysis of short-term pore pressure fluctuations in a thin colluvium landslide complex near Cincinnati, Ohio, Eng. Geol., 31, 159–184, 1991.
Hornberger, G. M., German, P. F., and Beven, K. J.: Throughflow and solute transport in an isolated sloping soil block in a forested catchment, J. Hydrol., 124, 81–99, 1991.
IA PAS: Manual for Field Operated Meter (FOM), Institute of Agrophysics, Polish Academy of Science Lublin, 34, 2006.
James, A. L. and Roulet, N. T.: Investigating the applicability of end-member mixing analysis (EMMA) across scale: A study of eight small, nested catchments in a temperate forested watershed, Water Resour. Res., 42, W08434, doi:10.1029/2005WR004419, 2006.
Jarvis, N. J.: A review of non-equilibrium water flow and solute transport in soil macropores: principles, controlling factors and consequences for water quality, Eur. J. Soil Sci., 58, 523–546, 2007.

ESURFD
1, 637–671, 2013

Field investigation of preferential fissure flow paths

D. M. Krzeminska et al.

Kabeya, N., Katsuyama, M., Kawasaki, M., Ohte, N., and Sugimoto, A.: Estimation of mean residence times of subsurface waters using seasonal variation in deuterium excess in a small headwater catchment in Japan, Hydrol. Process., 21, 308–322, 2007.
Kienzler, P. M. and Naef, F.: Temporal variability of subsurface stormflow formation, Hydrol. Earth Syst. Sci., 12, 257–265, doi:10.5194/hess-12-257-2008, 2008.
Kirchner, J. W.: A double paradox in catchment hydrology and geochemistry, Hydrol. Process., 17, 871–874, 2003.
Larsbo, M. and Jarvis, N.: Information content of measurements from tracer microlysimeter experiments designed for parameter identification in dualpermeability models, J. Hydrol., 325, 273–287, 2006.
Linsley, R. K., Kohler, M. A., and Paulhus, J. L. H.: Hydrology for Engineers, 3rd Edn., New York, McGraw-Hill Book Company, 1982.
Mali, N., Urbanc, J., and Leis, A.: Tracing of water movement through the unsaturated zone of a coarse gravel aquifer by means of dye and deuterated water, Environ. Geol., 51, 1401–1412, 2007.
Malet, J.-P.: Les glissements de type écoulement dans les marnes noires des Alpes du Sud. Morphologie, fonctionnement et modélisation hydro-mécanique, Ph.D. thesis, Université Louis Pasteur, Strasbourg, 2003.
Malet, J.-P., Maquaire, O., and Calais, E.: The use of Global Positioning System techniques for the continuous monitoring of landslides: application to the Super-Sauze earthflow (Alpes-de-Haute-Provence, France), Geomorphology, 43, 33–54, 2002.
Malet, J.-P., van Asch, Th. W. J., van Beek, R., and Maquaire, O.: Forecasting the behaviour of complex landslides with a spatially distributed hydrological model, Nat. Hazards Earth Syst. Sci., 5, 71–85, doi:10.5194/nhess-5-71-2005, 2005.
McDonnell, J. J.: The influence of macropores on debris flow initiation, Q. J. Eng. Geol. Hydroge., 23, 325–331, doi:10.1144/GSL.QJEG.1990.023.04.06, 1990.
Mikovari, A., Peter, C., and Leibundgut, Ch.: Investigation of preferential flow using tracer techniques, in: Tracer Technologies for Hydrological Systems, Proceedings of a Boulder Symposium, July 1995, 1995.
Mulholland, P. J. and Hill, W. R.: Seasonal patterns in streamwater nutrient and dissolved organic carbon concentrations: Separating catchment flow path and in-stream effects, Water Resour. Res., 33, 1297–1306, doi:10.1029/97WR00490, 1997.

ESURFD
1, 637–671, 2013

Field investigation of preferential fissure flow paths

D. M. Krzeminska et al.

Niethammer, U., James, M. R., Rothmund, S., Travelletti, J., and Joswig, M.: UAV-based remote sensing of the Super-Sauze landslide: Evaluation and results, Eng. Geol., 128, 2–11, doi:10.1016/j.enggeo.2011.03.012, 2012.

Pierson, T. C.: Soil pipes and slope stability, Q. J. Eng. Geol., 16, 1–15, 1983.

Savage, W. Z., Godt, J. W., and Baum, R. L.: A model for spatially and temporally distributed shallow landslide initiation by rainfall infiltration, in: Proceedings of the third international conference on debris flow hazards mitigation: mechanics, prediction, and assessment, edited by: Rickenmann, D. and Chen, C.-L., Davos, Millpress, Rotterdam, 2003.

Schulson, E. M. and Duval, P.: Creep and Fracture of Ice, Cambridge University Press, New York, 2009.

Šimůnek, J., Jarvis, N. J., van Genuchten, M. T., and Gardenas, A.: Review and comparison of models for describing non-equilibrium and preferential flow and transport in the vadose zone, J. Hydrol., 272, 14–35, 2003.

Sivapalan, M., Jothityangkoon, C., and Menabde, M.: Linearity and nonlinearity of basin response as a function of scale: discussion of the alternative definitions, Water Resour. Res., 38, doi:10.1029/2001WR000482, 2002.

Soulsby, C., Rodgers, P., Smart, R., Dawson, J., and Dunn, S.: A tracer-based assessment of hydrological pathways at different spatial scales in a mesoscale Scottish catchment, Hydrol. Process., 7, 759–777, doi:10.1002/hyp.1163, 2003.

Stumpf, A., Malet, J.-P., Kerle, N., Niethammer, U., and Rothmund, S.: Image-based mapping of surface fissures for the investigation of landslide dynamics, Geomorphology, 15, 12–27, 2012.

Travelletti, J., Sailhac, P., Malet, J.-P., Grandjean, G., and Ponton, J.: Hydrological response of weathered clay-shale slopes: water infiltration monitoring with time-lapse electrical resistivity tomography, Hydrol. Process., 26, 2106–2119, doi:10.1002/hyp.7983, 2012.

Trojan, M. and Linden, D.: Micro relief and rainfall effects on water and solute movement in eartchworm burrows, Soil Sci. Soc. Am. J., 56, 727–733, 1992.

Tromp-van Meerveld, H. J. and McDonnell, J. J.: Threshold relations in subsurface stormflow: 2. the fill and spill hypothesis, Water Resour. Res., 42, W02411, doi:10.1029/2004WR003778, 2006.

Uchida, T., Kosugi, K., and Mizuyama, T.: Effects of pipeflow on hydrological process and its relation to landslide: a review of pipeflow studies in forested headwater catchments, Hydrol. Process., 15, 2151–2174, 2001.

ESURFD

1, 637–671, 2013

Field investigation of preferential fissure flow paths

D. M. Krzeminska et al.

Walter, M., Arnhardt, C., and Joswig, M.: Seismic monitoring of rockfalls, slide quakes, and fissure development at the Super-Sauze mudslide, French Alps, Eng. Geol., 128, 12–22, 2012.
Weiler, M. and McDonnell, J. J.: Conceptualizing lateral preferential flow and flow networks and simulating the effects on gauged and ungauged hillslopes, Water Resour. Res., 43, W03403, doi:10.1029/2006WR004867, 2007.
Weiler, M. and Naef, F.: An experimental tracer study of the role of macropores in infiltration in grassland soils, Hydrol. Process., 17, 477–493, 2003.
Wienhöfer, J., Lindenmaier, F., and Zehe, E.: Challenges in Understanding the Hydrologic Controls on the Mobility of Slow-Moving Landslides, Vadose Zone J., 10, 496–511, doi:10.2136/vzj2009.0182, 2011.
Van Bavel, M. and Nichols, C.: Theta and Profiler Soil Moisture Probes – Accurate Impedance Measurement Devices – New Applications, Technical Report, 2002.
Van Beek, L. P. H. and van Asch, T. W. J.: A combined conceptual model for the effects of fissure-induced infiltration on slope stability, in: Process Modelling and Landform Evolution, edited by: Hergarten, S. and Neugebauer, H. J., Lecture Notes in Earth Sciences, 78, 147–167, doi:10.1007/BFb0009716, 1999.
Van Schaik, L.: The role of macropore flow from PLOT to catchment scale, Ph.D. thesis, in: Netherlands Geographical Studies, University of Utrecht, the Netherlands, 2010.
Zehe, E. and Fluhler, H.: Preferential transport of isoproturon at a plot scale and a field scale tile-drained site, J. Hydrol., 247, 100–115, 2001.

ESURFD
1, 637–671, 2013

Field investigation of preferential fissure flow paths

D. M. Krzeminska et al.

Table 1. Measured (^{m}) and estimated (^{e}) components of water balance for each plot, with the assumption that whole experience area is hydrological active.

	Plot A		Plot B		Plot C	
Day of experiment (duration)	1st (7 h)	2nd (8 h)	1st (7 h)	2nd (8 h)	1st (7 h)	2nd (7 h)
Assumed average porosity, n [–]	0.35	0.35	0.38	0.38	0.30	0.30
$^{(m)}$Initial average volumetric soil moisture, θ_{ini} [–]	0.12	0.12	0.25	0.27	0.23	0.25
$^{(e)}$Water in soil column, V_{PE} [m^3]	0.23	0.24	0.32	0.34	0.78	0.79
$^{(m)}$Sprinkling volume, P [m^3]	0.27	0.33	0.36	0.42	0.29	0.30
$^{(m)}$Overland flow, OF, [m^3]	Not observed		Not observed		0.22	0.23
$^{(e)}$Infiltrated water, V_{INF} [m^3]	0.27	0.33	0.36	0.42	0.09	0.08
$^{(e)}$Subsurface flow, (SSF) [m^3]	–*	0.23	0.34	0.41	0.09	0.008
– $^{(m)}$exfiltration [m^3]	Not observed		> 0.17**	0.30	Not observed	
$^{(e)}$Water in soil column, $V(t_{end})$ [m^3]	–*	0.34	0.35	0.35	0.79	0.79
$^{(e)}$Change in storage, ΔS [m^3]	–*	0.10	0.02	0.01	0.01	0.01
$^{(e)}$Final average volumetric soil moisture, $\theta(t_{end})$ [–]	–*	0.17	0.27	0.28	0.25	0.26

* Estimation not possible because of missing groundwater level observation.
** Exfiltration started after 2 h of sprinkling but was measured only since 3rd hour of sprinkling experiment.

ESURFD
1, 637–671, 2013

Field investigation of preferential fissure flow paths

D. M. Krzeminska et al.

ESURFD
1, 637–671, 2013

Field investigation of preferential fissure flow paths

D. M. Krzeminska et al.

Table 2. Measured (^{m}) and estimated (^{e}) tracer mass balance components and the evaluation of the hydrologicaly active area assumptions.

	Plot A		Plot B		Plot C	
Day of experiment (applied tracer)	1st (Br^-)	2nd (Cl^-)	1st (Br^-)	2nd (Cl^-)	1st (Br^-)	2nd (Cl^-)
Tracer in applied water – $^{(m)}$concentration, $[\,]_{EW}$ [g m^{-3}]	118	1035	122	128	123	1047
– $^{(e)}$mass [g]	32.3	343.7	44.1	53.5	35.6	322.5
$^{(e)}$infiltrated tracer [g]	32.3	343.7	44.1	53.5	10.1	82.5
assuming that whole area is hydrological active						
$^{(e)}$Tracer out of soil column via: – overland flow, [g]	Not observed		Not observed		22.3	237.3
– subsurface flow, [g]	–*	162.8	> 33**	36.2	4.2	2
$^{(e)}$Mass of tracer remained in soil column based on mass budget [g] ($mass_{in}$–$mass_{out}$)	–*	180.9	< 11.1	17.3	5.9	82.6
$^{(m)}$Tracer concentration in the groundwater, [ ] (t_{end}) [g m^{-3}]	91.4	768.5	81.4	73.6	45.8	50.34
$^{(e)}$Mass of tracer remained in soil column based on measured concentration, [g] ($V(t_{end}) \times [\,]\,((t_{end}))$	–*	261.3	27.7	25.8	35.7	39.7
assuming that x percentage of the area is hydrological active						
$^{(e)}$Percent of the plot area that is hydrologicaly active, x [%]	–*	53	24	60	17	210
$^{(e)}$Tracer out of the soil column via subsurface, [g]	–*	86.3	> 25.7**	34.2	0.7**	4.3
$^{(e)}$Mass of tracer remained in soil column based on mass budget [g]	–*	257.4	< 18.4**	19.3	9.4**	82.7
$^{(e)}$Mass of tracer remained in soil column based on measured concentration, [g]	–*	257.7	18.4	18.9	9.5	80.8

* Estimation/measurements not possible because of the missing groundwater level observation.
** Exfiltration started after 2 h of sprinkling but was measured only since 3rd hour of sprinkling experiment.

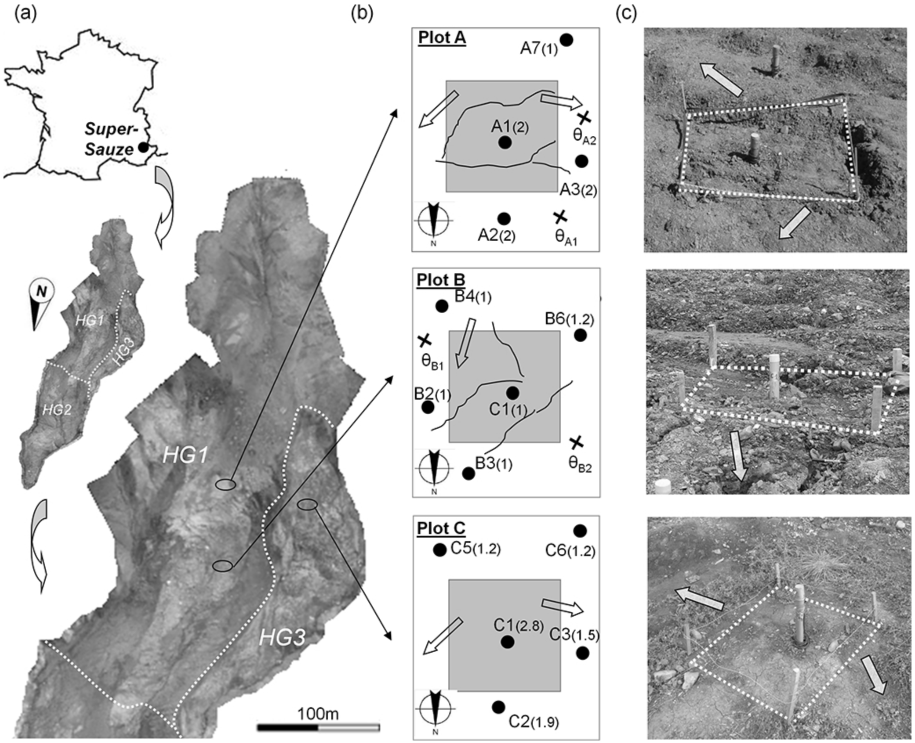

Fig. 1. (a) The upper part of the Super-Sauze landslide with indicated location of three sprinkling tests (plot A, B and C); the white dashed lines indicate the hydro-geomorphological units (after Malet et al., 2005). **(b)** Schematic representation of the experimental setup of each area (not scaled); grey squares represents $1 \times 1\,\mathrm{m}^2$ sprinkling plots; dots represent the location of the piezometers; numbers in brackets indicate the depth of the piezometers in metres; crosses indicate the location of the theta probes; undulating lines indicate fissure distribution within the sprinkling plots and arrows show the local slope direction in the area. **(c)** Photographs of the soil surface of each sprinkling area with arrows showing the local slope direction in the area.

ESURFD
1, 637–671, 2013

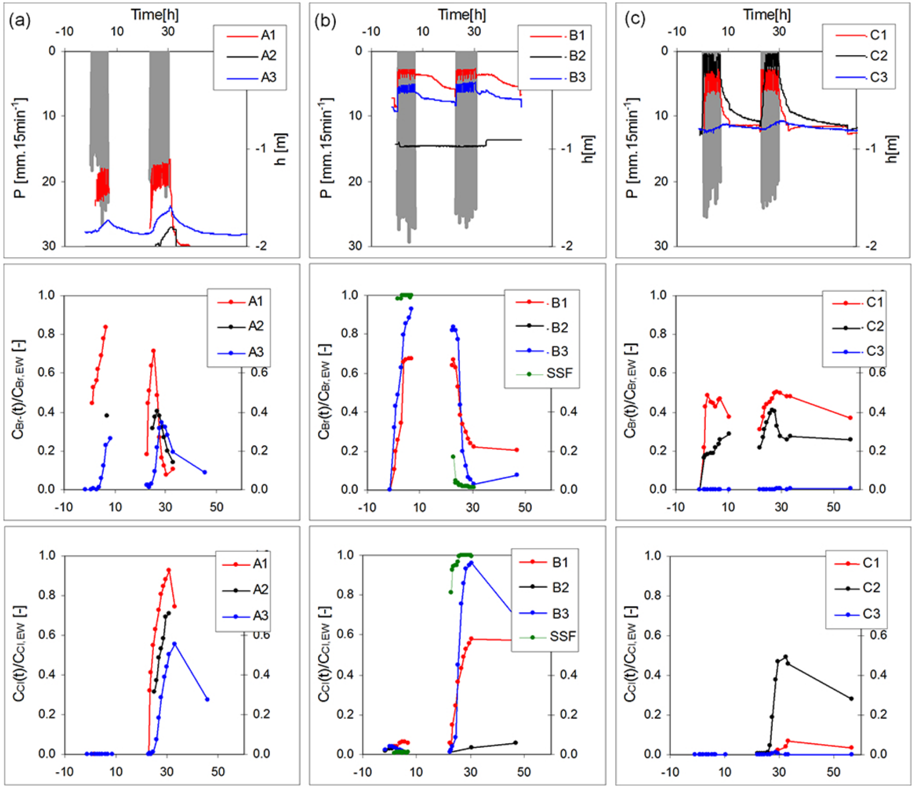

Fig. 2. Monitoring results of three sprinkling experiments: **(a)** plot A, **(b)** plot B and **(c)** plot C. Upper panels show the intensity of the sprinkling (primary *y* axis) and groundwater responses in piezometers (secondary *y* axis). Middle and bottom panels show the ratio between tracer concentration measured in the piezometers or subsurface runoff (SSF) and the applied tracer concentration.

ESURFD

1, 637–671, 2013

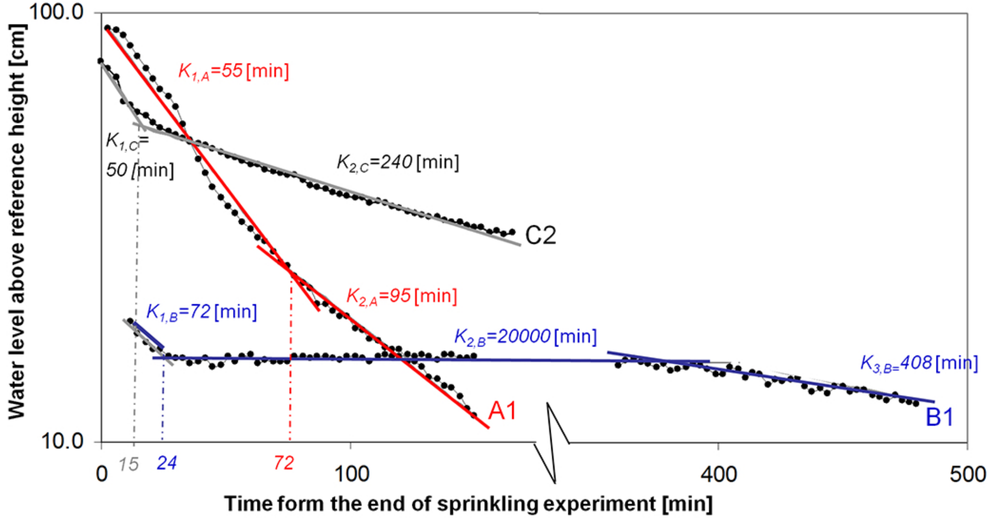

Fig. 3. Drawdown curves observed in piezometers A1, B1 and C2 after the end of sprinkling experiments and corresponding depletion factors *K* [min].

ESURFD

1, 637–671, 2013

Field investigation of preferential fissure flow paths

D. M. Krzeminska et al.

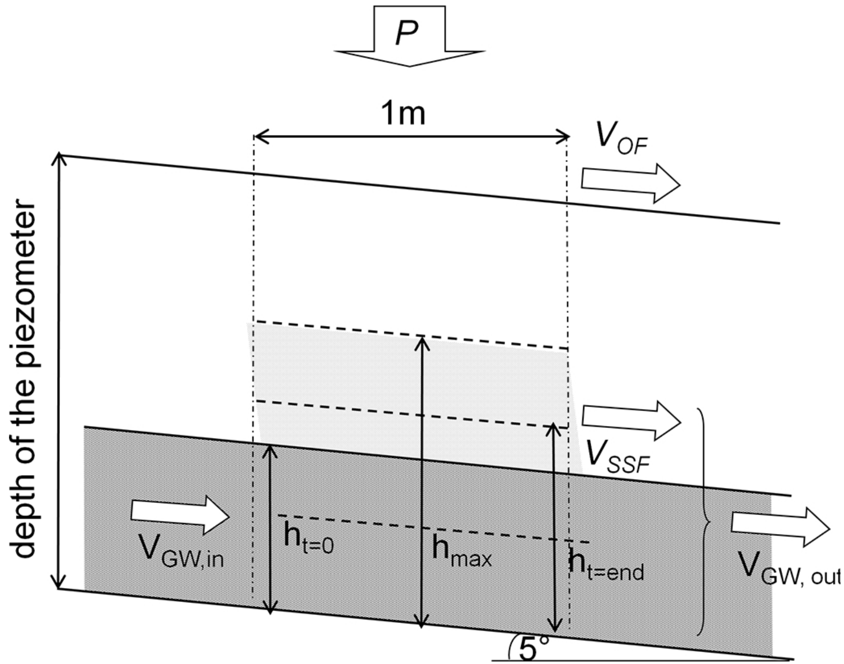

Fig. 4. Schematic representation of water balance components of experimental plots.

ESURFD
1, 637–671, 2013

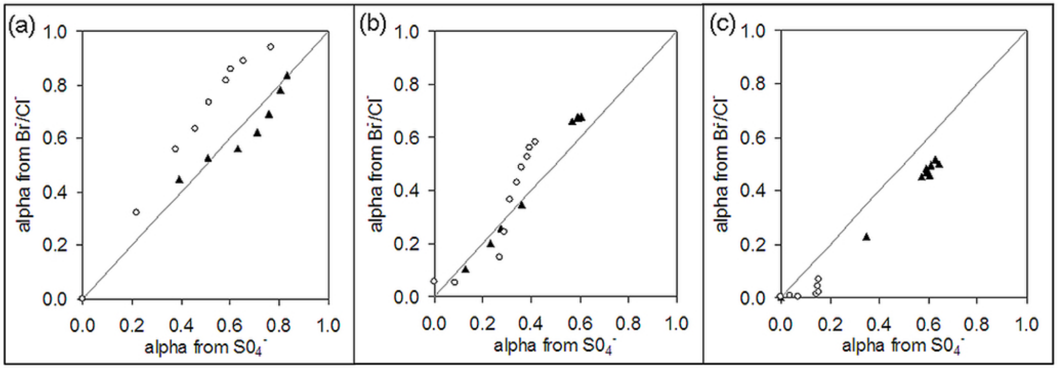

Fig. 5. EMMA model results for the centrally located piezometers A1 **(a)**, B1 **(b)** and C1 **(c)**. The full triangles are estimates for the first day of the experiment and the open dots represents second day of the experiment. The grey line is 1 : 1 line.

ESURFD
1, 637–671, 2013

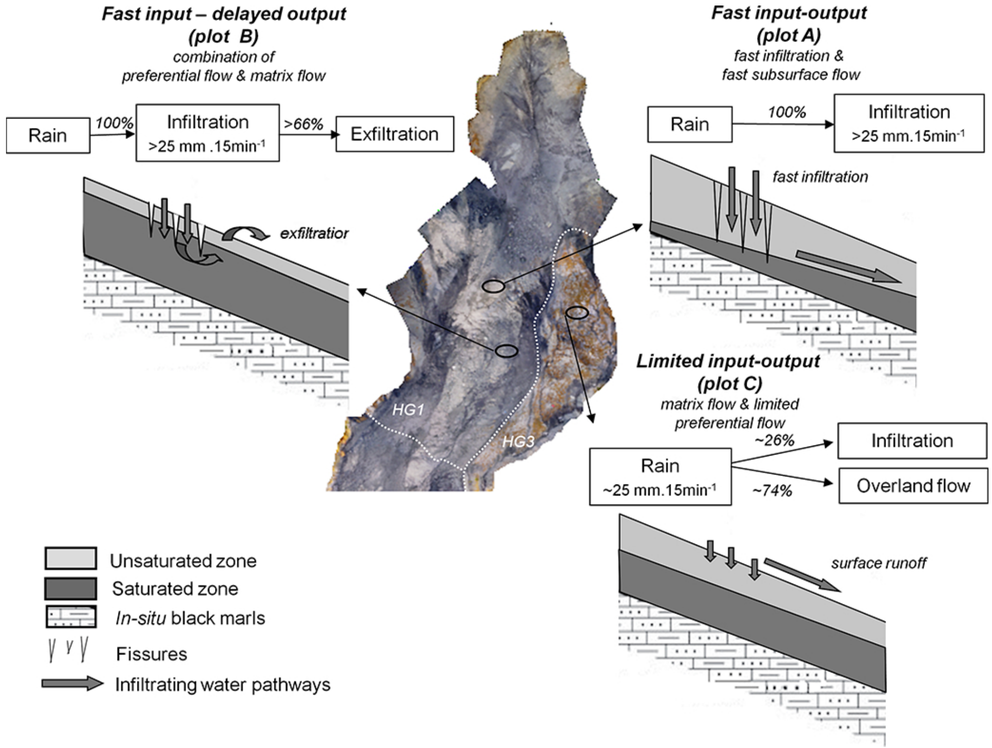

Fig. 6. Hydrological concepts derived from hydrological and hydrochemical analysis of small-scale sprinkling experiment and their distribution across the upper part of the Super-Sauze landslide. The white dashed lines indicate the hydro-geomorphological (HG) units defined by Malet et al. (2005).

ESURFD
1, 637–671, 2013